

Accepted Manuscript

Design and synthesis of disubstituted and trisubstituted thiazoles as multifunctional fluorophores with large Stokes shifts

Polina O. Suntsova, Alexander K. Eltyshev, Tatiana A. Pospelova, Pavel A. Slepukhin, Enrico Benassi, Nataliya P. Belskaya



PII: S0143-7208(18)32673-1

DOI: <https://doi.org/10.1016/j.dyepig.2019.02.051>

Reference: DYPI 7385

To appear in: *Dyes and Pigments*

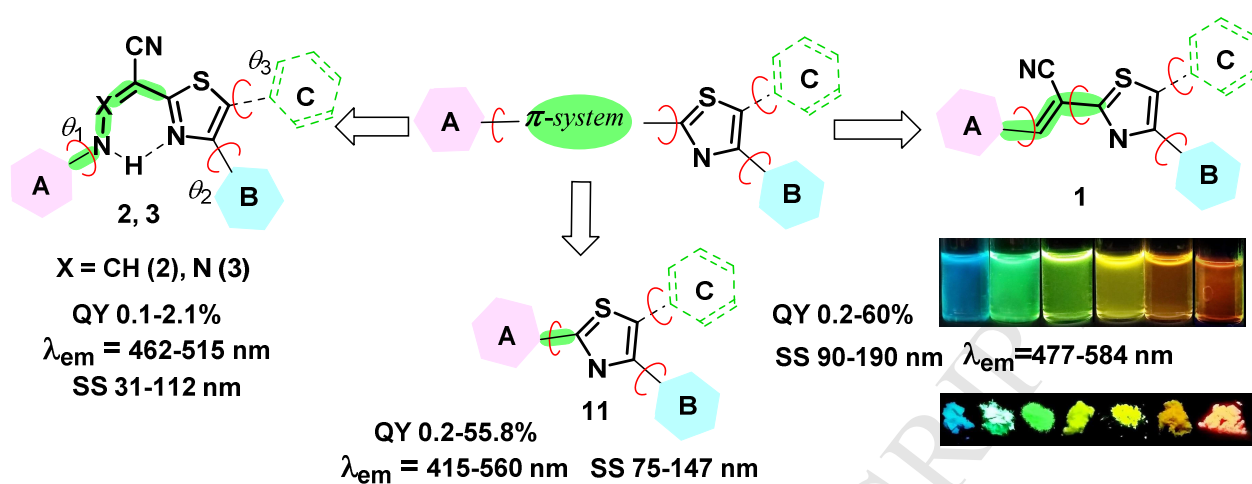
Received Date: 5 December 2018

Revised Date: 12 February 2019

Accepted Date: 28 February 2019

Please cite this article as: Suntsova PO, Eltyshev AK, Pospelova TA, Slepukhin PA, Benassi E, Belskaya NP, Design and synthesis of disubstituted and trisubstituted thiazoles as multifunctional fluorophores with large Stokes shifts, *Dyes and Pigments* (2019), doi: <https://doi.org/10.1016/j.dyepig.2019.02.051>.

This is a PDF file of an unedited manuscript that has been accepted for publication. As a service to our customers we are providing this early version of the manuscript. The manuscript will undergo copyediting, typesetting, and review of the resulting proof before it is published in its final form. Please note that during the production process errors may be discovered which could affect the content, and all legal disclaimers that apply to the journal pertain.



Design and Synthesis of Disubstituted and Trisubstituted Thiazoles as Multifunctional Fluorophores with Large Stokes Shifts

Polina O. Suntsova,^a Alexander K. Eltyshv,^a Tatiana A. Pospelova,^a Pavel A. Slepukhin,^{a,b} Enrico Benassi,^{*c} Nataliya P. Belskaya^{*a,b}

^a*Ural Federal University, 19 Mira Str., Yekaterinburg 620002, Russian Federation*

^b*Postovsky Institute of Organic Synthesis, Ural Branch of Russian Academy of Science, 22 S. Kovalevskaya Str., Yekaterinburg, 620219, Russian Federation*

^c*Department of Chemistry, Hexi University, Zhangye, 734000, PR of China*

*Corresponding authors: e-mail: n.p.belskaya@mail.ru, ebenassi3@gmail.com

Abstract

A series of fluorophores based on a thiazole core have been synthesized and shown to be very sensitive to both structural changes and the microenvironment. Simple modifications of the substituents' electronic nature, spatial effects and location in the molecule allow the tuning of the photophysical properties of the investigated compounds and their susceptibility to the environment via the exhibition of long-wavelength emission, large Stokes shifts and good quantum yields. Additionally, the thiazole-2-acrylonitrile fluorophores demonstrate a multifunctional character with significant fluorescence properties (i.e., quantum yields and a large Stokes shift in both the liquid and solid states). The influences of different factors, including the solvent polarity, on the fluorescence properties of the synthesized compounds are discussed in detail. Quantum mechanical methods are employed to understand the underlying transitions and explain the experimental results. This work provides further information for the design of new sensors that have large Stokes shifts.

Keywords: Thiazole, Arylidene, Fluorescence, Solvatochromism, Stokes Shift, Biosensor

1. Introduction

Substituted 1,3-thiazoles, as heterocyclic cores, are commonly found in nature and are a preferable structural fragments in various drugs [1]. Monocyclic thiazole is an essential motif of fluorescent molecules and can be used to construct multifunctional materials [2] and chemosensors [3]. Among the fluorescent thiazoles, 4-hydroxy- and 4-alkoxy derivatives are considered to be outstanding compounds. The structures of 4-hydroxy- and 4-alkoxy derivatives are very similar to that of luciferin of fireflies, and they have been shown to exhibit remarkable emission properties [4]. 2- or 5-aminoderivatives are another large group of thiazoles that have a large Stokes shift and long-wavelength emission independent of their molecular structure [5]. Numerous investigations have been devoted to the synthesis of fluorescent thiazoles, which have been demonstrated to have photophysical properties that are strongly dependent on the electronic nature of the substituents at the 2-, 4- and 5-

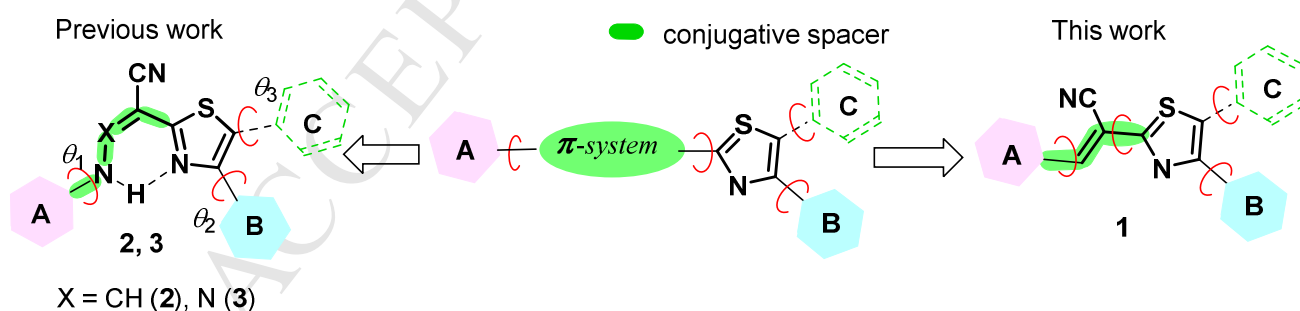
positions of the thiazole core and their combinations [4,5]. Some relationships between the structure and fluorescence were found for thiazoles containing additional aryl- or heteroaryl rings with various types of substituents. For example, Görls and co-workers [4c,d] showed that the combination of an electron-donor moiety (OH or OAlk) at the 5-position and an electron-acceptor moiety at the 2-position of the thiazole improved the charge-transfer character, which, therefore, increased the Stokes shift and led to a redshift in the fluorescence emission. Yashita and co-workers [5b] supported the conclusion that strong electron-accepting groups (4-NO₂C₆H₄, 4-CF₃C₆H₄) at the C2 thiazole atom can cause large bathochromic shifts in the emission wavelength. Takitoh and co-workers [5d] synthesised a series of 5-*N*-arylaminothiazoles, investigated their fluorescence and solvatochromic behaviour, and confirmed that the combination of electron-donating groups at the C5 thiazole ring (*N*-arylamino groups) and an electron-accepting aromatic ring at the C2-atom of the heterocycle core was optimal for shifting of the absorption and emission bands to longer wavelengths and that the 4-position had no essential influence on the photophysical characteristics. You X.-Z. and co-workers [5c] generated a family of linear symmetric and asymmetric D- π -A and D- π -D thiazoles and drew the same conclusions as mentioned above regarding the relationship of the structure-fluorescence characteristics. However, Hanusek J. and co-authors [4a] observed that changing the substituents in the aromatic ring in 5-arylthiazoles from an electron-donor to an electron-acceptor group did not substantially influence the fluorescence. In addition, it was shown that the 2-position of the thiazole ring was very sensitive to the microenvironment [5c]. All the presented results led to similar conclusions, and this knowledge about the optical properties of thiazoles can be considered to provide us with a good platform for the synthesis of fluorophores with tunable emission. However, Radhakrishnan and Sreejalekshmi [5a] carried out an extensive investigation on the photophysical properties of a 30-member library of thiazole-thiophene cores with an aromatic ring at the C4 position and a strong electron-accepting 5-nitrothiophene moiety at the C5 thiazole. The fluorescence characteristics of these library members were shown to have a strong dependence on the electronic nature of the C4 aromatic ring. They found that this type of electronic structure relied on a new additional channel (C4→C5) compared with the traditional channel (C5→C2). The results obtained in some cases were the opposite of the aforementioned conclusions: electron-accepting substituents at the C5-thiazole position were more important for colour tunability; the presence of electron-donating groups at C4 of thiazole induced a redshift, and the electron-donating groups of diphenylamine and dimethylaniline placed at C2 and C4 exhibited synergistic effects on the absorption and emission wavelengths, respectively [5a]. All these findings indicate the need to perform further investigations to examine the structure-photophysical properties of thiazoles for the future design of new fluorophores based on the thiazole core. In addition, the main published results concerning thiazoles have included high polar hydroxyl- or amino-groups or their derivatives with an extremely strong electron-donor

effect of the substituents and atoms, which can take part in strong intermolecular interactions as donors or acceptors of hydrogen bonds.

Another significant detail for the design of new fluorophores with long-wavelength emission is the molecular configuration, which may include various types of spacers (bonds, cyclic structures, and atoms) that bind the separate fragments/substituents/rings [6]. Various π - π linkers have been used to increase the conjugative system (double and triple bond, heterocycles, azo- or azine group) at the thiazole C5 atom [4c, 5g,i,k, 7]. Much less is known about the effect of linear or cyclic systems on extending the conjugation chain attached at the 2-position of thiazole [8].

Recently, we generated new thiazole derivatives, **2** and **3** (Scheme 1), with flexible conjugated linear systems involving enamine (**ETZs 2**) or aza-enamine (**ATZs 3**) side chains at the C2 ring atom and determined that the type of spacer group that links the thiazole to the peripheral aromatic ring is very important. For example, the Stokes shift of thiazoles **2** and **3** varies depending on the combination of the electronic and spatial effects of the substituents on the aromatic cycles (**A** and **B**) over a large range (31–112 nm / 1900–5500 cm⁻¹) [9].

The aim of this study was to investigate the fluorescence of fluorophores based on thiazole surrounded by two or three aromatic/heteroaromatic rings, with one of them (at the C2 atom) separated from the key heterocycle by an acrylonitrile fragment. The electronic structures of these compounds are tuned by the classical approach of coupling various combinations of the substituents (D(C4)- π -A(C2), A(C4)- π -D(C2), A(C4)- π -A(C2), D(C5)-D(C4)- π -A(C2) and D(C5)-A(C4)- π -A(C2)) as well their spatial parameters and locations within the aromatic rings **A**, **B** (at C4 thiazole ring) and **C** (at C5 atom thiazole). Several of the designed thiazoles did not include the C5 aromatic ring in their structure to define its significance on the photochemical behaviour of the investigated compounds.



Scheme 1. Design of new fluorophores based on thiazoles.

2. Experimental

2.1. Instruments and Materials

¹H NMR and ¹³C NMR, spectra were recorded with a Bruker Avance II (Karlsruhe, Germany) (400 MHz for ¹H, 100 MHz for ¹³C) spectrometer. Chemical shifts are reported in parts per million

(ppm) relative to TMS in ^1H NMR, to the residual solvent signals in ^{13}C as external reference. Coupling constants (J) values are given in Hertz (Hz). Signal splitting patterns are described as a singlet (s), doublet (d), triplet (t), quartet (q), sextet (sext), quintet (quin), multiplet (m), broad (br), doublet of doublets (dd), doublet of triplets (dt) or AA'XX' - spin system of para-substituted benzene with two different substituents. The ^{13}C NMR signal patterns for several compounds were analysed by APT (attached proton test). The major isomer signal is highlighted with an asterisk (*). Mass spectra were recorded with a Shimadzu GCMS-QP 2010 "Ultra" (Kyoto, Japan) mass spectrometer using the electron impact (EI) ionization technique (40-200 °C, 70 eV). The abbreviation $[\text{M}]^+$ refers to the molecular ion. Spectra of exact mass were acquire on a quadrupole orthogonal acceleration time-of-flight mass spectrometer (Synapt G2 HDMS, Waters, Milford, MA). Samples were infused at 3 $\mu\text{L}/\text{min}$ and spectra were obtained in positive (or: negative) ionization mode with a resolution of 15000 (FWHM) using leucine enkephalin as lock mass. The Fourier-transform infrared (FT-IR) spectra were obtained using a Bruker Alpha (NPVO, ZnSe) spectrometer (Ettlingen, Germany). Elemental analyses were carried out using a CHNS/O analyzer Perkin-Elmer 2400 Series II instrument (Shelton, CT USA). Melting points for compounds **1a-q,u**, **2a,b**, **3a,b**, **4d**, **7a,b**, **8a**, **9a** were determined on a Stuart SMP3 apparatus (Staffordshire, ST15 OSA, UK) for compounds **1r,t,v,w** were determined using method of Differential scanning calorimetry (Mettler-Toledo DSC822e module).

X-ray crystallographic analysis was performed with a Xcalibur diffractometer with CCD using a standard procedure (MoK-irradiation, graphite, ω -scanning with step 1°). CCDC-1872988 (for **1c**) is given in the ESI and supplementary crystallographic data for this paper. These data can be obtained free of charge from the Cambridge Crystallographic Data Centre via www.ccdc.cam.ac.uk/data_request/cif.

UV-Vis absorption spectra were recorded on a Perkin-Elmer Lambda 35 UV-Vis spectrophotometer (Shelton, CT USA). Fluorescence of the sample solutions was measured using a Hitachi F-7000 spectrophotometer (Tokyo, Japan). The absorption and emission spectra were recorded in toluene, dioxane, CH_2Cl_2 , CHCl_3 , THF, EtOH, EtOAc, acetone, MeCN, DMF, DMSO using 10.00 mm quartz cells. The excitation wavelength was at the absorption maxima. Atmospheric oxygen contained in solutions was not removed. Concentration of the compounds in the solution was 5.0×10^{-5} M and 5.0×10^{-6} M for absorption and fluorescence measurements, respectively. The relative fluorescence quantum yields (Φ_{F}) were determined using quinine sulfate in 0.1 M H_2SO_4 as a standard ($\Phi_{\text{F}} = 0.546$). Absolute quantum yield for solid state and time-resolution study were recorded on Horiba FluoroMax 4 Spectrofluorometer (Kyoto, Japan) with Quanta- ϕ integrating sphere using FluorEssence 3.5 Software.

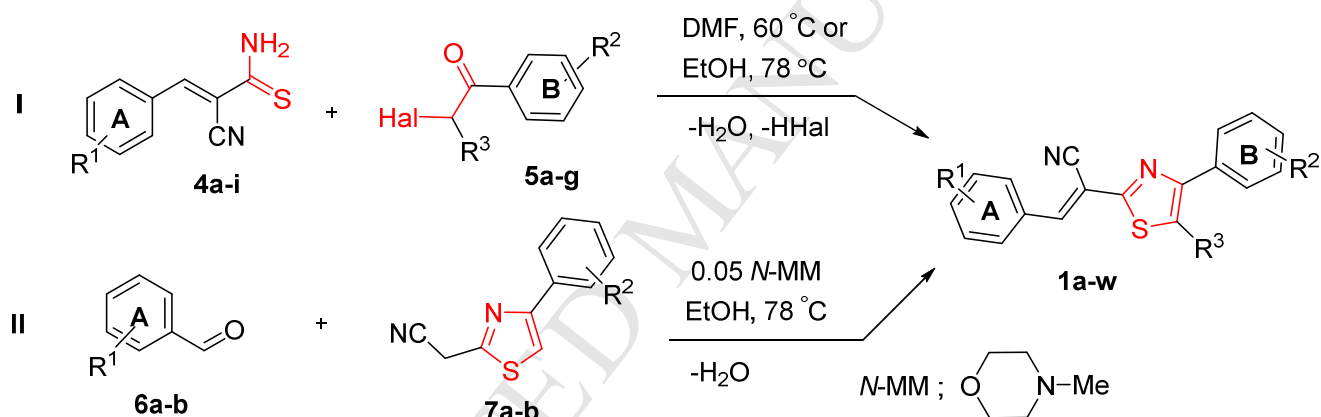
The reactions were monitored by analytical thin-layer chromatography (TLC) on aluminium-backed silica-gel plates (Sorbfil UV-254). Visualization of components was accomplished by short wavelength UVlight (254 nm). Solvents were dried and distilled according to the common procedures.

All solvents were of spectroscopic grade. Full experimental details for the synthesis of compounds **1a-w**, **2a,b**, **3a,b**, **4d**, **7a,b**, **8a** and **9a** as well as their NMR spectra, photophysical characterization, and quantum mechanical calculation data are reported in the electronic Supplementary information (ESI).

2-Cyanoethanethioamide, halocarbonyl compounds **5a-g** and arylaldehydes **6a,b** were obtained from Acros Organics and used without further purification.

Arylidenethioamides **4a-i**, arylhydrazonothioacetamide **8a** and arylaminothioacrylamide **9a** were prepared according to procedures reported in the literature and their spectral characteristics were identical to the published data [9,10]. Thiazoles **11** were prepared according to procedures reported in the literature and their NMR, IR, and mass-spectrometry data were identical to the published data [11, 12].

2.2. General synthetic procedures for thiazoles **1a-w** (Scheme 2).



4 A = 4-MeOC₆H₄ (**a**), 4-ClC₆H₄ (**b**), 4-CF₃C₆H₄ (**c**), 4-CNC₆H₄ (**d**), 4-NO₂C₆H₄ (**e**), Pyridin-4-yl (**f**), 2-ClC₆H₄ (**g**), 2,4-Cl₂C₆H₃ (**h**), 2,6-Cl₂C₆H₃ (**i**)

5 Hal = Br R³ = H, R² = 4-MeO (**a**); 4-Cl (**b**); H (**c**); R³ = Ph, R² = H (**d**), 4-Cl (**e**); R³ = 4-MeC₆H₄ R² = H (**f**); Hal = Cl R³ = MeOC₆H₄ R² = 4-MeOC₆H₄ (**g**)

6 R¹ = 4-CF₃C₆H₄ (**a**), Pyridin-4-yl (**b**)

7 R² = 4-MeO (**a**), 4-Cl (**b**)

Scheme 2. Synthesis of ATAs **1a-w**.

Method A Halocarbonyl compound **5** (1.0 mmol) was added to a solution of thioamide **4** (0.9 mmol) in dimethylformamide (DMF; 1.0 mL) or ethanol (EtOH; 1.0 mL) for compounds **1r,t,m**. The mixture was stirred at 60 °C for 0.5–24.0 h until the thin layer chromatography (TLC) analysis indicated total consumption of the starting thioamide. The resulting mixture was diluted with EtOH (1.0 mL) and cooled in an ice-salt bath for 1 h. The precipitate was collected by filtration, washed with water-ethanol solution (20 mL, 1 : 1), and dried.

Method B. Aldehyde **6** (2.4 mmol) and *N*-methylmorpholine (0.01 mL, 0.1 mmol) were added to a solution of thiazole **7** (2.0 mmol) in DMF (2.0 mL). The mixture was stirred at 60 °C for 1.5–2.5 h until the TLC analysis indicated total consumption of the starting thiazole. The resulting mixture was diluted with ethanol (2.0 mL) and cooled in an ice-salt bath for 1 h. The precipitate was collected by filtration, washed with water-ethanol solution (20 mL, 1 : 1), and dried.

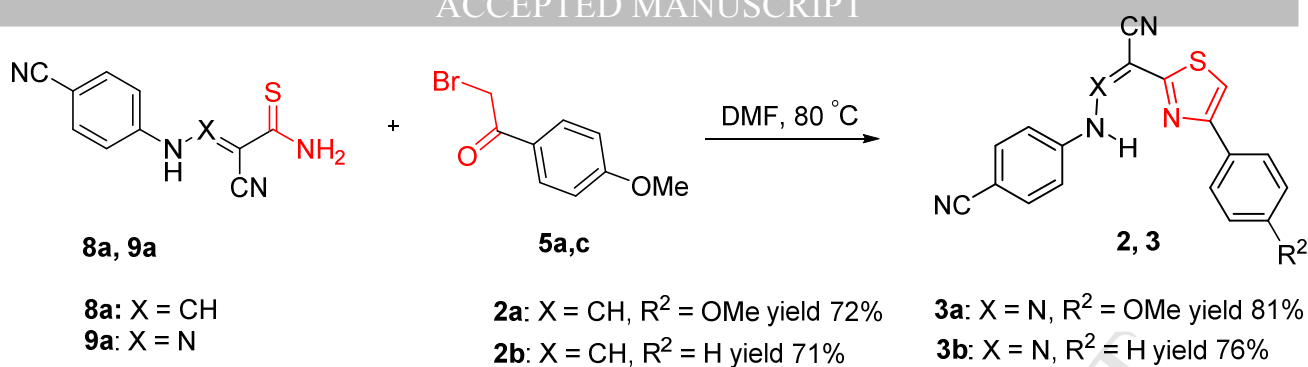
Table 1. Time for the conversion of compounds **4a–i** in reaction with halocarbonyl compounds **5a–g** and aldehydes **6a–b** condensation with thiazoles **7a–b** and yields of ATAs **1a–w**

Entry	Compd	Structure			Time, (h)	Yield, ^a (%)	Route
		A	R ²	R ³			
1	1a	4-MeOC ₆ H ₄	4-MeO	H	5.0	86	I
2	1b	4-MeOC ₆ H ₄	4-Cl	H	3.0	88	I
3	1c	4-ClC ₆ H ₄	4-MeO	H	3.0	80	I
4	1d	4-ClC ₆ H ₄	H	H	1.0	91	I
5	1e	4-CF ₃ C ₆ H ₄	4-MeO	H	6.0	62	II
6	1f	4-CF ₃ C ₆ H ₄	4-Cl	H	3.5	78	II
7	1g	4-CNC ₆ H ₄	4-MeO	H	3.5	80	I
8	1h	4-CNC ₆ H ₄	H	H	1.5	92	I
9	1i	4-CNC ₆ H ₄	4-Cl	H	1.0	97	I
10	1j	4-NO ₂ C ₆ H ₄	4-MeO	H	3.0	82	I
11	1k	4-NO ₂ C ₆ H ₄	H	H	2.0	85	I
12	1l	Pyridin-4-yl	4-MeO	H	1.5	56	II
13	1m	Pyridin-4-yl	H	H	2.0	63 ^b	I
14	1n	Pyridin-4-yl	4-Cl	H	2.5	80	II
15	1o	2-ClC ₆ H ₄	4-MeO	H	24.0	70	I
16	1p	2,4-Cl ₂ C ₆ H ₃	4-MeO	H	2.0	65	I
17	1q	2,6-Cl ₂ C ₆ H ₃	4-MeO	H	4.0	80	I
18	1r	4-ClC ₆ H ₄	4-MeO	4-MeOC ₆ H ₄	8.0	63 ^c	I
19	1s	4-ClC ₆ H ₄	H	Ph	5.0	79	I
20	1t	4-CNC ₆ H ₄	4-MeO	4-MeOC ₆ H ₄	1.0	88 ^c	I
21	1u	4-CNC ₆ H ₄	H	Ph	7.0	52	I
22	1v	4-CNC ₆ H ₄	4-Cl	4-MeC ₆ H ₄	20.0	62	I
23	1w	4-CNC ₆ H ₄	4-Cl	Ph	23.0	93	I

^a Isolated yields after separation and purification. ^b Condensation thioamide **4f** with 2-bromo-1-phenylethan-1-one **5c** under reflux in EtOH. ^c Reaction conditions: reflux thioamides **4b,d** with 2-chloro-1,2-diphenylethan-1-one **5g** in EtOH.

2.3. General synthetic procedure for ETZs **2** and ATZs **3** (Scheme 3).

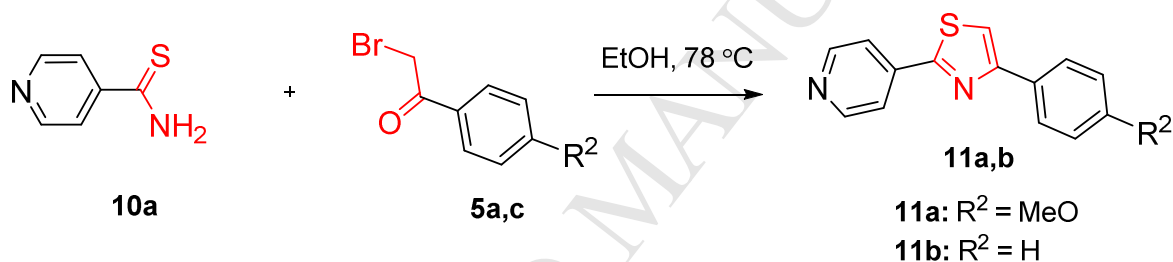
Enaminethiazoles **2** and azaenaminethiazoles **3** were prepared according to procedures reported in the literature [9]. Halocarbonyl compound **5** (1.0 mmol) was added to a solution of thioamide **8a** or **9a** (0.9 mmol) in DMF (1.0 mL). The mixture was stirred at 80 °C for 4 h until the TLC analysis indicated total consumption of the starting compound. The resulting mixture was diluted with ethanol (1.0 mL) and cooled in an ice-salt bath for 1 h. The precipitate was collected by filtration, washed with water-ethanol solution (20 mL, 1 : 1), and dried.



Scheme 3. Synthesis of **ETZs 2a,b** and **ATZs 3a,b**.

2.4. General procedure for the synthesis of thiazoles **11** (Scheme 4).

Thiazoles **11a,b** were prepared according to procedures reported in the literature [11, 12]. Halocarbonyl compound **5** (1.0 mmol) was added to a solution of a pyridine-4-thioamide **10a** (0.9 mmol) in EtOH (1.0 mL) for compounds **1r,t,m**. The resulting mixture was cooled in an ice-salt bath for 1 h. The precipitate was collected by filtration and dried.



Scheme 4. Synthesis of thiazoles **11a,b**.

3. Result and discussion

2.1. Synthesis and characterization

To realize our desired goals, we attempted to employ a simple synthetic method to introduce various combinations of substituents into the thiazole core. Syntheses of 3-aryl-2-(thiazol-2-yl)acrylonitriles (**ATAs**) **1a–w** were carried out according to the *Hantzsch* thiazole synthesis, in which thioacetamides **4a,b,d,e,g,h,i** were condensed with the opportune α -halocarbonyl compounds **5a–g** in DMF, while the reactions of thioamides **4b,d,f** with 2-bromo-1-phenylethan-one **5c** or 2-chloro-1,2-diphenylethan-1-one **5g** used ethanol (Table 1, entries 13, 18, 20) [9, 10]. The choice of solvent was determined based on the solubility of substrates **4** and **5**. The desired products **1a–d,g–k,m,o–w** were obtained after a single purification step with good overall yields (63–97%). The results are summarized in Table 1. However, in the reaction of thioamides **4c,f** with bromoacetophenones **5a,b**, the products **1e,f,l** and **n** were scarcely obtained; instead of route I, they were synthesized at good yields by another route (II) based on the reaction of the aldehydes **6a,b** with the thiazoles **7a,b** [11].

The synthetic procedures used for the preparation of the designed molecules are simple, efficient, and sustainable. The important advantage of the classical *Hantzsch* synthesis is the probability of

obtaining a large and diverse library of desirable compounds from inexpensive and available starting materials. Furthermore, two rings can be simultaneously attached onto C4 and C5 atoms of thiazole by using suitable 2-bromo(chloro)-1,2-diarylethan-1-ones. An alternative method, the palladium-catalysed cross-coupling reaction, requires the additional steps of constructing the starting thiazole ring, followed by this parent core being pre-functionalized with a halogen or metal at the position where the aryl groups should be attached [4d, 13]. Sometimes, pre-functionalization by bromination or chlorination leads to the formation of by-products that bear an additional halogen atom owing to the presence of electron-donating substituents at the aryl group favouring their formation. Thus, the thiazoles **1r** and **1t** could not be obtained by this cross-coupling procedure.

The structures for **ATAs 1a–w** were confirmed by Fourier-transform infrared spectroscopy (FTIR), ^1H nuclear magnetic resonance (NMR) spectroscopy, ^{13}C NMR spectroscopy, mass spectrometry and elemental analysis data. The details of the experimental procedures and data for structural characterization are provided in the electronic supplementary information (ESI). Notably, the NMR spectra show that compounds **1a–w** each exist as one steric isomer (Figs. S1–23, ESI). Additionally, the crystal structure of **1c** was determined by single-crystal X-ray diffraction (XRD) analysis. XRD quality crystals were grown from ethanol with slow evaporation at room temperature. The representative bond lengths and torsion angles are presented in Fig. S33 (ESI), and the crystal structure is shown in Fig. 1.

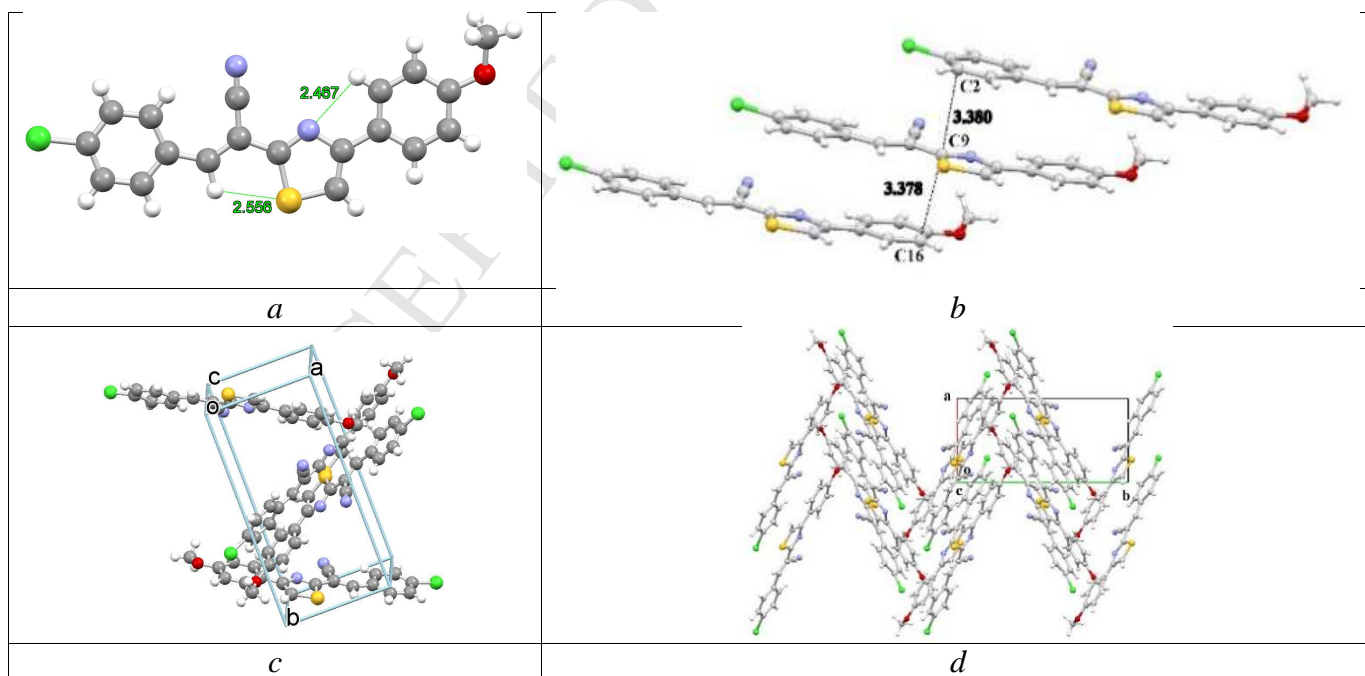


Fig. 1. (a, b) Crystal structure of the compound **1c** and (c, d) the crystal packing diagram.

The results indicate that the compound crystallized in the monoclinic system with the $P2_1/c$ space group. The molecule is essentially planar and exists as an *E* geometric isomer with respect to the C1–C2 double bond.

It is known that molecular packing plays a significant role in the photoluminescence efficiency [6, 14]. *J*- and *X*-stacking are preferable for increasing the emission intensity [15]. As shown in Fig. 1, the molecules of **ATA 1c** were packed into parallel two-dimensional sheets (Fig. 1*b*), in which all of the neighbour molecules were located in a head-to-tail arrangement. Adjacent sheets in the single-crystal adopted a rotational angle of approximately 58° (Fig. 1*c*). In the crystal, packing molecules were partly linked through intermolecular π - π interactions, which resulted in parallel stacking, and all of the molecules were shifted with respect to each other. The perpendicular distance between the closest sheets was 3.380 Å (Fig. 1*b*), and only weak interactions between the dye layers were expected [16]. The dipoles of the two molecules of compound **1c** facing each other head-on in the same sheet (Fig. 1*c*) opposed each other. Consequently, the presence of excited state deactivation channels by internal conversion and a subsequent radiation less decay to the electronic ground state (GS) is unlikely. Thus, the crystal packing may be classified as being close to *J*-type, which explains the emission in the solid state (vide infra).

2.2. Photophysical properties of ATAs

With the 23-member library of the synthesized **ATAs 1a–w** in hand, we estimated their photophysical properties to validate their potential for use as fluorophores. Fig. 2 shows photographs of solutions of **1a–w** in acetonitrile (MeCN) under irradiation with UV light; the corresponding data are listed in Table 2. Compounds **1a**, **1b** and **1d** were non-fluorescent.



Fig. 2. Photographs of solutions of **1a–w** in acetonitrile under irradiation with a hand-held UV lamp at an emission wavelength of 365 nm.

Synthesized thiazoles exhibited substantial shifts in their absorption wavelength in the range of 357–407 nm, with a large range of values for the extinction molar coefficients ($\epsilon_{\text{max}} = 7300\text{--}29200 \text{ M}^{-1} \text{ cm}^{-1}$). The displacement of the electron-accepting NO_2 - or CN -group at ring **A** instead of the electron-donating MeO -group in combination with the 4- MeO -substituent ring **B** or rings **B** and **C** simultaneously led to bathochromic shifts in the long wavelength absorption bands (Table 2, Entries 1, 10 and 20). Despite consideration of the whole set of absorption bands for the obtained compounds, the influence of the electronic effects of the substituents is not obvious.

Table 2. Photophysical data of **ATAs 1a–w** in solution (MeCN)

Entry	Compd	UV-Vis ^a		Fluorescence ^b		Stokes shift (nm/cm ⁻¹)	$\langle\tau\rangle_f^e$ (ns)
		$\lambda_{abs},^c$ (nm)	$\epsilon_{max},$ (M ⁻¹ cm ⁻¹)	$\lambda_{em},$ (nm)	$\Phi_F,^d$ (%)		
1	1a	380	17800	-	-	-	-
2	1b	373	23300	472	0.2	99/5620	-
3	1c	376	11900	543	4.8	167/8180	3.61
4	1d	364	29200	480	0.3	116/6640	-
5	1e	380	10200	555	1.5	175/8300	-
6	1f	359	12000	490	5.7	131/7450	1.20
7	1g	389	7300	561	0.8	172/7880	1.43
8	1h	370	16200	501	18.0	131/7070	3.40
9	1i	367	11200	501	18.0	134/7290	2.85
10	1j	399	11700	-	-	-	-
11	1k	382	19100	552	5.1	170/8060	2.85
12	1l	382	9000	561	4.0	179/8350	1.92
13	1m	361	7600	495	26.3	134/7300	4.85
14	1n	357	8900	495	16.8	138/7810	4.24
15	1o	372	9000	555	6.2	183/8860	3.93
16	1p	377	9600	557	3.1	180/8570	3.05
17	1q	360	8600	550	3.8	190/9600	4.07
18	1r	394	16200	553	6.2	159/7300	3.63
19	1s	365	13600	501	0.4	136/7440	-
20	1t	407	14500	572	7.8	165/7090	2.9
21	1u	379	16800	527	10.1	148/7410	3.20
22	1v	383	12200	535	11.0	152/7420	3.02
23	1w	377	13100	522	11.4	145/7370	2.48

^a Absorption measured in solution with a sample concentration of 5×10^{-5} M. ^b Emission measured at a sample concentration of 5×10^{-6} M. ^c Longest absorption maxima are only reported. ^d Fluorescence quantum yields (QYs) are measured relative to quinine sulfate ($\lambda_{exc} = 366$ nm; $\Phi = 0.53$). ^e Fluorescence lifetime.

Dilute solutions of compounds **1a–w** showed emission bands centred with maxima over a large wavelength range from 472 to 572 nm; the data also demonstrated a strong dependence on the substituent combination at rings **A**, **B**, and **C** and their locations. The increase in the electron-accepting properties of the ring **A** substituents and decrease in the electron-accepting properties of the ring **B** substituents caused a bathochromic shift in the fluorescence maxima of up to 561 nm (89 nm) for diaryl-substituted **ATA 1g**. Introduction of the additional aromatic ring **C** to the C5 atoms of thiazoles **1r–w** afforded an additional shift in the emission maxima to the red region (10–26 nm), especially for **ATAs 1r** and **1t**, which had electron-donating substituents on rings **B** and **C**; at the same time, this increased their quantum yields (Table 2, entries 3, 7, 18, and 20). It should be mentioned that the introduction of a second 4-methoxyphenyl moiety at the C5 position of the thiazole ring resulted in a redshift of 18 nm and 11 nm in the absorption and emission bands, respectively (Table 2, entries 7 and 20). This behaviour may originate from the strengthening of the electronic coupling between the donor and acceptor terminals of the molecule through the thiazole moiety and the acrylonitrile π -spacer. Appearance of a second shorter conjugation system, in accordance with that established by

Radhakrishnan and Sreejalekshmi [5a], but with the opposite direction (C5→C4), may be the reason for the larger long-wavelength shifts of 24 and 21 nm observed for compounds **1w** and **1v**, respectively (Table entries 9, 22 and 23). Thus, a combination of substituents D(C5)-A(C4)-A(C2) supported the possibility of a new intramolecular charge transfer (ICT) strengthening (C5→C4) as well as (C4→C5) [5a], which can be used for the design of new effective fluorophores with a long-wavelength emission.

It should be noted that the emission characteristics depend on the location of the substituent on the aromatic ring **A**. For example, displacement of the Cl atom from the 4- to the 2-position on ring **A** led to a small redshift of the long-wavelength maxima (12 nm). This change was opposite to the blue shift of the absorption maxima (4 nm) (Table 2, entry 3 and 15). However, the efficiency of fluorescence of the 2-substituted compounds **1o-q** increased because of the reduction in the non-radiative emission owing to the spatial hindrances caused by rotating ring **A**.

The steric bulkiness (ring **A**) and increasing conjugation along C4 also had noticeable effects on the emission, as evident from a comparison of the spectra of the 4-aryl-substituted thiazoles **1c,d,g,h,i** and 4,5-diaryl-substituted thiazoles **1r,w**. Compounds **1a-w** had fluorescence quantum yields (QYs) that increased from 0.2 to 26.3% in acetonitrile (relative to quinine sulphate).

Thus, modification of every thiazole substituent (C2, C4 and C5 atoms) was identified to be crucial for the π -conjugation network and, consequently, for manipulating the **ATAs** by a push-pull effect.

We should emphasize that the main feature of the photophysical properties of the thiazoles obtained was their remarkable Stokes shifts, which reached up to 9600 cm^{-1} (190 nm) in acetonitrile (Table 2, entry 17). In addition, this is one of the largest values reported for Stokes shifts for both thiazoles [4,5] and organic fluorophores in principle [17]. Furthermore, despite the considerable Stokes shift, the **ATAs** retained quite significant values for the QY compared with examples in the literature, as an increase in the Stokes shift usually results in a sharp drop in the quantum yield [4,5]. For example, **ATAs 1a-w** in acetonitrile had an increased Stokes shift from 131 to 190 nm, which was accompanied by a 7-fold decrease in the QY (from 27.2 to 3.8%), while 5(5-nitrothiophene-2-yl)thiazoles [5a] showed an 84-fold drop in the QY (8.4 to 0.1%) with a similar change in the Stokes shift (129–195 nm).

Fluorescence lifetime decay measurements of the thiazole solutions in acetonitrile were performed (Table 2, Table S1, ESI). Fig. S35 (ESI) illustrates the excited-state decay curves for the dyes recorded in acetonitrile. The detailed data for the corresponding decay parameters are included in Table S1 (ESI). In acetonitrile, thiazole had fluorescence lifetimes in the range of 1.20–5.30 ns. Importantly, the pyridyl-derivatives of **1m** and **1n** possessed the longest average fluorescence lifetimes, which indicated that they exhibited some of the best fluorescence properties, consistent with the absorption and emission spectra. The values of the radiative (k_r) and non-radiative decay constant (k_{nr}) of the thiazoles in acetonitrile were calculated [6]. The larger non-radiative decay constant values of **ATAs**

1g and **1f** demonstrated the dominant dissipation of excitation energy through non-radiative channels (Table S1, ESI).

2.3. Solvato (fluoro) chromism

Compounds **1c,g,h,k–n,u** were studied in different solvents (hexane, toluene, CH₂Cl₂, EtOH, *i*-PrOH, acetone, DMF, acetonitrile, DMSO, 1,4-dioxane, CHCl₃, *n*-BuOAc, EtOAc) in aerated solutions at room temperature. The strong influences of the electronic effect of the substituents in the molecules and the polarity of the solvents on the photophysical properties were demonstrated. The solvatochromic and solvatofluoric properties of the ATAs **1c,g,h,k–n** and **u** are summarized in Fig. 3, Fig. S37 and Table S2 (ESI).

The absorption spectra of the thiazoles **1c,h,k–n,u** showed little dependence on the solvent polarity. By contrast, solvent-dependent bathochromic shifts of more than 60 nm (60–97 nm) were observed in the fluorescence spectra. Normalized emission spectra are shown in Fig. 3 and in Figs. S37 and S38 (ESI). As the solvent became polar, the emission exhibited increasing redshifts, indicating an ICT behaviour, which is better stabilized in polar solvents. The observations outlined above suggest emission from ICT, which seemed to have a greater dipole moment in the excited state than in the GS. ATA **1k** was more sensitive to the solvent polarity and demonstrated the largest shift to longer wavelengths (97 nm).

The QY of **1c,g,h,k–n,u** in various solvents revealed that the fluorescence intensity was very strongly dependent on the structure and solvent used. The studied thiazole derivatives can be divided into three groups. The first group includes ATAs **1k** and **1l**, which showed a more intense emission in non-polar CH₂Cl₂ or toluene. Their structures included strong electron-accepting substituents at the arylacrylonitrile fragment at the C2 atom and electron-donor groups at the aryl cycle at the C4 atom of the thiazole ring. The second group involves compounds **1c** and **1h**, which have better fluorescence intensity in more polar solvents, such as acetone or DMF. Finally, the third group includes ATAs **1m**, **1n**, and **1u**, for which the largest QY values were observed in alcohols (EtOH, *i*-PrOH). The most intense emissions were obtained for thiazole **1m** in EtOH (60%). The large values of the QY in alcohols for thiazoles **1m**, **1n**, and **1u** suggested their strong potential to form intermolecular hydrogen bonds, which decreased the molecular rotations during geometric relaxation and decreased the non-radiative processes for energy loss. These findings [18] regarding the formation of intramolecular non-covalent bonding, owing to dipole-dipole interactions or hydrogen bond formation, promote the use of such compounds as chemo-sensors and bio-sensors.

Analysis of the Stokes shift values in different solvents for the investigated molecules (Fig. 3 and additional spectra in Fig. S37, ESI) showed large Stokes shift values for most of the compounds. The large increase in the values of the Stokes shift followed the increase in the solvent polarity, as demonstrated for the compounds **1c,h,k–n,u** in acetone, MeCN, DMF and DMSO, with values in the

range of 127–179 nm. The high Stokes shift is very useful for small organic fluorophores [6, 17], especially for their imaging applications [19].

More evidence that the strong ICT behaviour was correlated with the large difference in dipole moments between the ground and excited states was the pronounced positive solvatochromism exhibited by all of the molecules studied (Table S2). For example, in the case of **1c**, upon increasing the solvent polarity from *n*-hexane to DMSO, the emission band was redshifted by 83 nm (468 nm in *n*-hexane and 551 nm in DMSO, Table S2). Such a high sensitivity to the microenvironment is comparable to the sensitivity of oxythiazoles and aminothiazoles, which have heteroatoms that are capable of forming intramolecular interactions [4a,e,g,j, 5a].

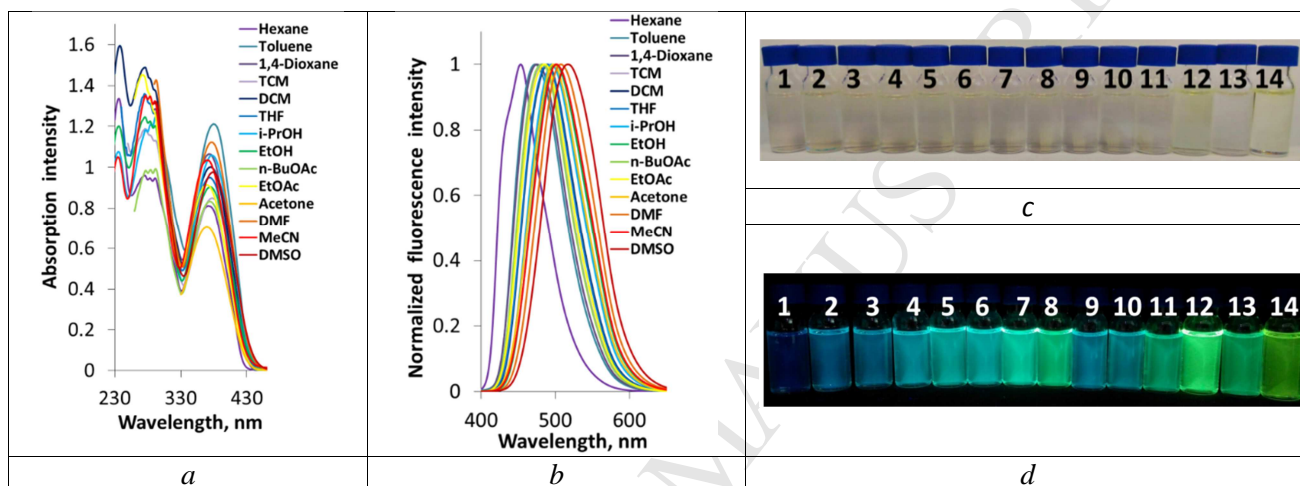





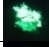

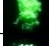



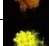



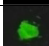



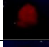

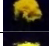

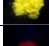
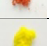
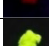



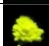







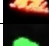




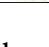

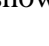
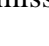


Fig. 3. (a) Absorption and (b) fluorescence spectra of **ATA 1h** in different organic solvents. For absorption measurements, **1h** concentration: 5×10^{-5} M, for fluorescence spectra, concentration: 5×10^{-6} M, excitation wavelength: 377 nm. Photographs of solutions of **ATA 1h** in acetonitrile under daylight (c) and under irradiation (d) with a hand-held UV lamp at an emission wavelength of 380 nm. Solvents: 1 – Hexane, 2 – Toluene, 3 – 1,4-Dioxane, 4 – CHCl_3 , 5 – CH_2Cl_2 , 6 – THF, 7 – *i*-PrOH, 8 – EtOH, 9 – *n*-BuOAc, 10 – EtOAc, 11 – Acetone, 12 – DMF, 13 – MeCN, 14 – DMSO.

2.4. Fluorescence of ATAs in the solid state

The crystal compounds of the thiazoles **1a–w** were yellow and bright-orange coloured. In addition to the photophysical properties shown in Table 4, we found that **ATAs 1a–w** exhibited solid-state fluorescence (Table 3, Fig. S40, ESI). All the dyes emitted at 477–584 nm with quantum yields in the range of 0.1–19.2%. The emission maxima of the solid samples of all of the studied **ATAs** were redshifted with respect to those of the corresponding solutions from 6 to 89 nm (Tables S3 and 4). The value of the QY in the solid state largely depended on the interactions between the molecules in the crystal packing, which was predicted and discussed above. It should be noted that the efficiency of the emission in the solid is very close to that of hydroxy- and aminothiazoles [4a, 5b].

ACCEPTED MANUSCRIPT

Table 3. Photophysical data of thiazoles **1a–w** in the solid state

Entry	Compd	λ_{ex} , (nm)	$\lambda_{\text{em.solid}}^a$, (nm)	Stokes shift (nm/cm ⁻¹)	Φ_s , ^b (%)	Photograph of powders	
						day light	UV-irradiation ^c
1	1a	380	526	146/7300	7.2		
2	1b	373	501	128/6850	19.2		
3	1c	376	522	146/7440	9.8		
4	1d	364	505	141/7670	11.3		
5	1e	380	537	157/7690	3.5		
6	1f	359	477	118/6890	5.2		
7	1g	389	528	139/6770	12.8		
8	1h	370	503	133/71506	2.8		
9	1i	367	521	154/8050	15.2		
10	1j	399	572	173/7580	0.1		
11	1k	382	545	163/7830	0.6		
12	1l	382	530	148/7310	0.8		
13	1m	361	584	223/10580	-		
14	1n	357	516	159/8630	3.2		
15	1o	372	519	147/7610	9.3		
16	1p	377	526	149/7510	13.6		
17	1q	360	509	149/8130	1.3		
18	1r	394	523	129/6260	7.7		
19	1s	362	495	133/7420	3.0		
20	1t	407	583	176/7420	2.6		
21	1u	379	506	127/6620	1.6		
22	1v	383	549	166/7890	6.1		
23	1w	377	523	146/7400	8.7		

^a Excited at $\lambda_{\text{ex.solid}}$. ^b Absolute fluorescence quantum yield. ^c Photographs showing the emission colours of **ATAs** solids when excited with a UV lamp ($\lambda_{\text{ex}} = 365$ nm).

2.5. Quantum mechanical calculations

To gain a better understanding of the nature of the electronic transitions underlying the absorption and fluorescence spectra, quantum mechanical methods were used. The **ATAs 1a–d,g–p,s,u** were first optimized in their ground electronic state (S_0) and lowest lying excited singlet electronic state (S_1) at the (TD-)DFT level (the details of the quantum mechanical calculation are presented in the ESI).

The structures of the **ATAs 1a–d,g–p,s,u** had several isomers/rotamers, which were at equilibrium. To determine the lowest energy structures for the investigated compounds, a conformational study was performed, which accounted for solvent (acetonitrile) effects. However, the differences in energies for the **ATAs 1a–d,g–p,s,u** between the different

conformers were small at room temperature, which meant that the observed properties and characteristics were average (Table S3, ESI). Therefore, in further computational investigations, we had to account for several more stable isomers/rotamers. The bond lengths, bond angles, and dihedral angles responsible for the photophysical parameters are listed in Tables S4–S11 (ESI). The structure of the **ATAs** in both the ground and excited states was found to be distorted from planarity (in acetonitrile). The dihedral angle θ_1 formed by ring **A** and the linear spacer of the dyes **1a–d,g–p,s,u** was a twisted angle, which showed values of up to 33.7° for the 4-substituted derivatives **1a–d,g–p,s,u** and 57.5° for the 2-substituted **ATA 1p** in the GS, which remarkably dropped (1.3 – 9.7°), even for the 2-substituted **1p**, in their excited state (Tables S5, S6, ESI). The alignment of ring **B** deviated from planarity with the thiazole plane by up to 17.9° for the 4-arylthiazoles **1a–d,g–p** and 40.8° for the diarylthiazoles **1s** and **1u** in the GS. In the excited states, the torsion angle θ_2 decreased to 2.7 – 15.8° for the 4-arylthiazoles and only changed to 3.9 – 7.3° for the 4,5-disubstituted derivative **1p**. Thus, the excited state geometries for the **ATAs 1a–d,g–p** became more planar compared with their geometries in the GS, apart from compound **1a**, for which the structure was twisted in the excited state owing to the increased torsion angle C1C2C3C5. The rotation of the aromatic ring **A** can cause a significant energy loss and lack of fluorescence. The conjugated system for most **ATAs** became stronger during excitation due to the shortening of the single bond lengths in S_1 (Tables S4 and S6, (ESI)). These data explain the insignificant influence of solvents on the **ATAs** absorption and the strong increasing of the polar solvent effect on their emission. However, the results of the geometry optimization showed some differences with the planarity observed in the single-crystal structure, which may be explained by the strengthening of the intermolecular interaction in the solid state.

The vertical excitations, major transitions of the absorption maxima, orbital contributing to the major transition for absorption, emission wavelength maxima, and their respective Stokes shifts were calculated using TD-DFT with the Polarizable Continuum Model (PCM in various solvents for the stable isomers). There was a good correlation between the experimental and calculated absorption and emission data (Tables S12, S13, ESI).

For compounds **1a–d,f**, excitation to the first singlet excited state ($S_0 \rightarrow S_1$) was preferable ($f_{01} = 0.3901 - 1.0853$, $\lambda_{\max} = 361$ – 392 nm). Then, the **ATAs** underwent the reverse transition, $S_1 \rightarrow S_0$, which was accompanied by emission ($f_{10} = 0.5113$ – 1.2076 , $\lambda_{\max} = 470$ – 561 nm) (Table S12, ESI). The dipole moment of the dyes **1a–b,g–p,s,u** showed that the push-pull dye **1j** had the largest dipole moment in the GS, which increased during the excitation (Tables S12, S13, ESI). The dipole moments of most of the investigated compounds remarkably increased in the vertical excited state, particularly for the **ATAs 1b,c,l,o,p,u**. Moreover, for the **1u** **A** and **B** rotamers, the dipole moment increased from the GS (10.7 D) to the Frank-Condon state by up to 16.7 D and after geometric relaxation became 17.8

D. Moreover, for **ATA 1u**, the increase of the dipole moment was accompanied by a substantial change in the angle of the dipole moment vector (up to 164.8–165.1° in S_{1r} (Table S12, ESI)).

The contour plots for the HOMO and LUMO levels of the dyes are presented in Fig. S44 (ESI). The electron densities in the HOMO and LUMO were dependent on the substitution pattern and its localization in the molecule. We classified these behaviour into two types: in the first type, the electron density was distributed almost evenly throughout the whole molecule for the **ATAs 1a–c,s,u** in the GS and for **1i–k,m–p,s,u** in the excited state. For the second type, the main part of the electronic density was localized on the ethylene link, thiazole ring and cycle **B** or the two cycles together (**B** and **C**). This pattern was observed for the compounds **1g,h–p**. In the LUMO, the electron density of all of the molecules was completely localized on the aromatic cycle **A**, thiazole ring, and linear double bond, while aromatic ring **B** at the 4- or cycles **B** and **C** at the 4- and 5-carbon atoms of thiazole were excluded from the common molecule conjugated system. This result indicated that the electron cloud was mainly concentrated on thiazole and cycle **A** and almost absent on the aromatic cycle **B** or **B** and **C** simultaneously. Thus, we concluded that rearrangement of the charge within the molecule takes place when the molecule absorbs a quantum of light.

The molecular electrostatic potential (MEP) provides important information about the molecular polarity in GS and ES and the probability of the intermolecular interactions, particularly dipole-dipole and hydrogen bonding interactions and changes of the molecular polarity during the excitation. It is understood from the MEP map that remarkable changes were accomplished by the transitions of the molecules of the **ATAs 1a,b,j–p** to the excited state. These changes are an additional explanation of their high sensitivity to the microenvironment in the excited state discussed above.

2.6. Influence of the acrylonitrile spacer on the photophysical properties of **ATAs**

To identify the role of the C2 acrylonitrile unit on the optical characteristics of the **ATAs**, we replaced this link with another: for example, a hydrazone or enamine unit (Scheme 3). Thus, the new compounds **2a,b** and **3a,b** were synthesized using a previously published procedure [9], and their photophysical properties were measured and compared with those of the **ATAs 1g** and **1h** (Table 4).

It was obvious that changing the hydrazono- and enamino-linkers in **EATs 2** and **AATs 3** to an acrylonitrile fragment led to a sharp enhancement of the photophysical properties of **ATAs**. We observed substantial increases in QY, as well as bathochromic shifts of the absorption and emission maxima and increased Stokes shifts.

Table 4. Absorption and emission properties of thiazoles **2a,b** and **3a,b** in different solvents

Entry	Compd	Solvent	UV-Vis		Fluorescence		Stokes shift, (nm/cm ⁻¹)
			λ_{abs} , (nm)	ϵ_{max} , (M ⁻¹ cm ⁻¹)	λ_{em} , (nm)	Φ_{F} , (%)	
1	1g	Toluene	400	11000	519	24.8	119/5730
2		DCM	396	8600	554	6.5	158/7200
3		EtOH	395	5100	555	0.8	160/7300
4		DMF	395	11000	570	0.2	175/7770
5		MeCN	389	7300	561	0.8	172/7880
6	1h	Toluene	380	17300	472	9.8	92/5130
7		CH ₂ Cl ₂	375	15700	490	13.1	115/6260
8		EtOH	375	12900	500	18.0	125/6670
9		DMF	376	17600	507	27.2	131/6870
10		MeCN	370	16200	501	18.0	131/7070
11	2a	Toluene	381	20500	441	0.3	60/3570
12		DCM	379	17300	447	0.1	68/4010
13		EtOH	378	9000	444	0.1	66/3930
14		DMF	380	31300	453	0.3	73/4240
15		MeCN	376	32300	451	0.1	75/4420
16	2b	Toluene	377	29800	438	<0.1	61/3690
17		DCM	375	30200	437	<0.1	62/3780
18		EtOH	373	20700	434	<0.1	61/3770
19		DMF	376	29900	436	<0.1	60/3660
20		MeCN	372	34700	-	-	-
21	3a	Toluene	405	24100	494	0.2	89/4450
22		DCM	404	18400	527	0.2	123/5780
23		EtOH	403	9400	508	0.2	120/5700
24		DMF	481	27900	-	-	-
25		MeCN	401	30500	505	0.1	104/5100
26	3b	Toluene	401	24700	490	<0.1	104/5100
27		DCM	399	21000	492	<0.1	93/4700
28		EtOH	398	23700	486	<0.1	88/4500
29		DMF	477	27400	-	-	-
30		MeCN	396	26900	-	-	-

^a Absorption measured in solution of concentration 5×10^{-5} M. ^b Emission measured at a sample concentration of 5×10^{-6} M. ^c Longest absorption maxima are only reported. ^d Quantum yields (QYs) are measured relative to quinine sulfate ($\lambda_{\text{exc}} = 366$ nm; $\Phi = 0.53$).

To determine the importance of the acrylonitrile linker on the photoactive ability, additional reference compounds were used, the thiazoles **11a,b**, which did not include this fragment but contained pyridine rings connected with the C2 atom thiazole ring by a σ -bond. The data for the absorption and emission characteristics of these compounds are absent in the literature; therefore, we synthesized these compounds and measured their absorption and emission spectra (Table 5).

Table 5. Absorption and emission properties of ATAs **11,m** and thiazoles **11a,b** in different solvents

Entry	Compd	Solvent	UV-Vis		Fluorescence		Stokes shift, (nm/cm ⁻¹)
			λ_{abs} , (nm)	ϵ_{max} , (M ⁻¹ cm ⁻¹)	λ_{em} , (nm)	Φ_F , (%)	
1	11	Toluene	392	9700	501	28.5	109/5550
2		CH ₂ Cl ₂	389	7900	542	12.9	153/7260
3		EtOH	392	8900	559	0.2	167/7620
4		DMF	388	10200	559	1.6	171/7880
5		MeCN	382	9000	561	4.0	179/8350
6		DMSO	390	8500	561	3.8	171/7820
7	11m	Toluene	372	10200	463	34.6	91/5280
8		CH ₂ Cl ₂	418	10300	554	8.6	136/5870
9		EtOH	370	9200	501	60.0	131/7070
10		DMF	368	8700	499	40.6	131/7130
11		MeCN	361	7600	495	26.3	134/7500
12		DMSO	371	7100	510	12.4	139/7350
13	11a	Toluene	340	3900	415	3.7	75/5300
14		CH ₂ Cl ₂	401	3100	548	8.9	147/6700
15		EtOH	340	5000	457	22.0	117/7500
16		DMF	340	4400	451	15.8	111/7200
17		MeCN	394	6300	560	0.2	166/7500
18		DMSO	341	5400	455	16.3	114/7300
19	11b	CH ₂ Cl ₂	376	5100	472	28.0	96/5400
20		EtOH	325	5900	407	4.8	82/6200
21		DMF	323	5200	402	4.1	79/6100
22		MeCN	370	9000	498	55.8	128/6900
23		DMSO	325	4500	-	-	

^a Absorption measured in solution of concentration 5×10^{-5} M. ^b Emission measured at a sample concentration of 5×10^{-6} M. ^c Longest absorption maxima are only reported. ^d Quantum yields (QYs) are measured relative to quinine sulfate ($\lambda_{\text{exc}} = 366$ nm; $\Phi = 0.53$).

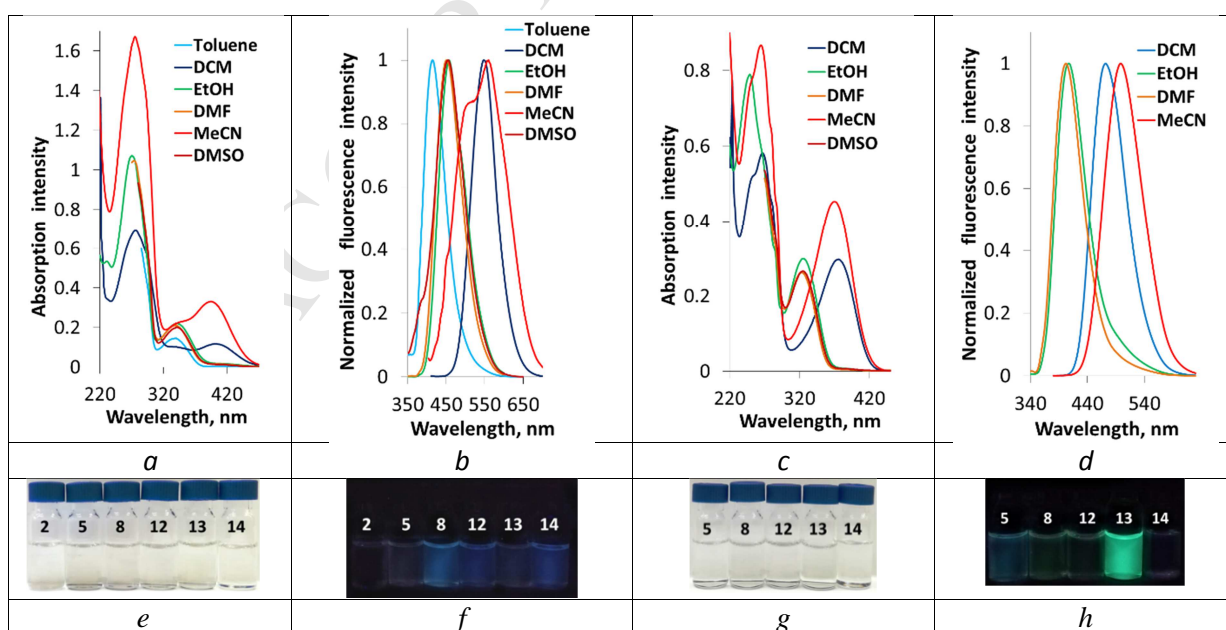


Fig. 4. (a, e, i, m, q, u) Absorption and (b, f, j, n, r, v) fluorescence spectra of ATAs **11a,b** in different organic solvents. For the absorption measurement, the sample concentration was 5×10^{-5} M. For the

fluorescence spectra, the sample concentration was 5×10^{-6} M with an excitation wavelength of 377 nm. Photographs of solutions of **ATAs 11a,b** under daylight (*c, j, k, o, s, x*) and under irradiation (*d, h, l, p, t, y*) with a hand-held UV lamp at 365 nm. 1 – Hexane, 2 – Toluene, 3 – 1,4-Dioxane, 4 – CHCl_3 , 5 – CH_2Cl_2 , 6 – THF, 7 – *i*-PrOH, 8 – EtOH, 9 – *n*-BuOAc, 10 – EtOAc, 11 – Acetone, 12 – DMF, 13 – MeCN, 14 – DMSO.

First, we should mention that compounds **11a,b** had lower solubility in organic solvents, as we used a smaller set of solvents for the investigation. The spectral data from a dilute sample in different solvents demonstrated large differences to the absorption and emission maxima of the thiazoles **11,m** and **11a,b**: (1) the **ATAs 11** and **1m** exhibited a more obvious bathochromic shift in absorption (48–52 nm for **11a** and 9–46 nm for **11b**); (2) compounds **11** and **1m** had larger Stokes shifts (91–829 and 1050–1848 cm^{-1} for **11a** and **11b**, respectively). Thus, the **ATAs 1** possesses the advantage of a relatively wide and adjustable range of fluorescence colours; (3) The **ATAs** maintained a remarkable emission intensity despite exhibiting large Stokes shifts. (4) The diversity in the structures of these two thiazole types resulted in the rather different behaviours observed in solvents. For example, the largest value of the QY for the **ATAs 11m** was obtained in ethanol (60%), while thiazole **11b** had the highest QY (55.8%) in acetonitrile. Thus, we can conclude that the most important factor for high-intensity and long-wavelength emission is the combination of an electron withdrawing substituent at the periphery of the C2 structural fragment with the electron donating substituent on the C4 aromatic cycle. In contrast to the results reported by Radhakrishnan and Sreejalekshmi [5a], the key influence of the C5 electron-accepting group was demonstrated for the case of the **ATAs 1**, for which good and rich photophysical characteristics were found for compounds where the C5 substituent was absent or had an electron-donating nature. It is obvious that the acrylonitrile spacer in the **ATA** structures plays an important role in their solvato (fluoro) chromic behaviour.

3. Conclusions

We described the synthesis, structures, and photophysical properties of a series of arylidenethiazoles **ATAs 1a–w** containing different types of substituents (electron-withdrawing and electron-donating groups) on each benzene ring for which the fluorescence properties were previously unknown in the literature. Despite the absence in their structures, polar substituents such as OH- or amino groups demonstrated high photophysical properties. Furthermore, **ATAs** showed multifunctional properties and exhibited fluorescence both in dilute solutions of different organic solvents and in the solid state with good or high quantum yields, large Stokes shifts, and relatively long lifetimes, which supports their potential for use as good fluorophores.

The obtained compounds demonstrated a strong effect of the electronic nature of the substituents on their fluorescence properties, in accordance with the previous literature data for the structure-

fluorescence relationship. In addition to these data, we showed the possibility of involving two ICT channels in a molecule and the ability to handle their strength and direction.

One of the main conclusions that can be drawn is that including an acrylonitrile spacer at the C2 thiazole position has a significant effect that governs the optical properties; in particular, this fragment changed the solvato (fluoro) chromic behaviour of thiazoles. In addition, our studies showed that this group enhances the sensitivity of the thiazole molecule to the microenvironment at a large scale; thus, they can be proposed for use as chemo- and biosensors. Studies on the further enhancement of the optical properties of these thiazoles are currently in progress.

Conflicts of interest

The authors declare no competing financial interest.

Acknowledgements

The reported study was funded by RFBR according to the research project No. 18-33-00859 mol_a. The Siberian Branch of the Russian Academy of Sciences (SB RAS) Siberian Supercomputer Center is gratefully acknowledged for providing supercomputer facilities. E.B. acknowledges the participation of undergraduate students Mr A. Karymsakov, Ms Zh. Mukanova, Ms G. Nurdildayeva, Mr M. Segizbayev, and Mr A. Shakenov (Dept of Chemistry, School of Science and Technology, Nazarbayev University, Astana, Rep. of Kazakhstan) for the preliminary quantum mechanical calculations.

Appendix A. The electronic supplementary material is available free of charge:

¹H and ¹³C NMR spectra of all new compounds; X-ray crystallographic data for compound **1c** (CCDC 1872988); Computational results and Cartesian coordinates (PDF).

References

- [1] (a) Manjal SK, Kaur R, Bhatia R, Kumar K, Singh V, Shankar R, Kaur R, Rawal RK. Synthetic and medicinal perspective of thiazolidinones: A review. *Bioorganic Chemistry* 2017;75:406-423. <https://doi.org/10.1016/j.bioorg.2017.10.014> (b) Zhang HZ, Gan LL, Wang H, Zhou CH. New Progress in Azole Compounds as Antimicrobial Agents. *Mini-Rev Med Chem* 2017;17:122-166. <https://doi.org/10.2174/1389557516666160630120725> (c) Jin Z. Muscarine, imidazole, oxazole and thiazole alkaloids. *Nat Prod Rep* 2011;28:1143-1191. <http://dx.doi.org/10.1039/C8NP00041G> (d) Arora P, Narang R, Nayak SK, Singh SK, Judge V. 2,4-Disubstituted thiazoles as multitargeted bioactive molecules. *Med Chem Res* 2016;25:1717-1743. <https://doi.org/10.1007/s00044-016-1610-2> (e) Martorana A, Giacalone V, Bonsignore R, Pace A, Gentile C, Pibiri I, Buscemi S, Lauria A, Piccionello AP. Heterocyclic Scaffolds for the Treatment of Alzheimer's Disease. *Curr Pharm Des* 2016;22:3971-3995. <https://doi.org/10.2174/1381612822666160518141650>
- [2] For recent reviews, see: (a) Yang Z, Cao J, He Y, Yang JH, Kim T, Peng X, Kim JS. Macro-/micro-environment-sensitive chemosensing and biological imaging. *Chem Soc Rev* 2014;43:4563-

4601. <https://doi.org/10.1039/C4CS00051J> (b) Pradhan T, Jung HS, Jang JH, Kim TW, Kang C, Kim JS. Chemical sensing of neurotransmitters. *Chem Soc Rev* 2014;43:4684-4713. <https://doi.org/10.1039/C3CS60477B> (c) Zhou Y, Zhang JF, Yoon J. Fluorescence and Colorimetric Chemosensors for Fluoride-Ion Detection. *J Chem Rev* 2014;114:5511-5571. <https://doi.org/10.1021/cr400352m> (d) Kaur P, Singh K. Supramolecular analyte recognition: experiment and theory interplay. *RSC Adv* 2014;4:11980-11999. <https://doi.org/10.1039/C3RA46967K> (e) Ghale G, Nau WM. Dynamically Analyte-Responsive Macrocyclic Host-Fluorophore Systems. *Acc Chem Res* 2014;47:2150-2159. <https://doi.org/10.1021/ar500116d> (f) Terenzi A, Lauria A, Almerico AM, Barone G. Zinc complexes as fluorescent chemosensors for nucleic acids: new perspectives for a “boring” element. *Dalton Trans* 2015;44:3527-3535. <https://doi.org/10.1039/C4DT02881C> (g) Zhou X, Lee S, Xu Z, Yoon J. Recent Progress on the Development of Chemosensors for Gases. *Chem Rev* 2015;115:7944-8000. <https://doi.org/10.1021/cr500567r>
- [3] (a) Sunguineti A, Sassi A, Turrise R, Ruffo R, Vaccaro R, Meinardi F, Beverina I. High Stokes shift perylene dyes for luminescent solar concentrators. *Chem Commun* 2013;49:1618-1620. <https://doi.org/10.1039/C2CC38708E> (b) Turrise R, Sunguineti A, Sassi M, Savoie B, Takai A, Patriaca GE, Salomone MM, Ruffo R, Vaccaro G, Meinardi F, Marks TJ, Facchetti A, Beverina IJ. Stokes shift/emission efficiency trade-off in donor-acceptor perylenemonoimides for luminescent solar concentrators. *Mater Chem A* 2015;3:8045-8054. <https://doi.org/10.1039/C5TA01134E>
- [4] (a) Kammel R, Tarabova D, Vana J, Machalicky, Nepras M, Hanusek J. Structure-fluorescence relationships in 2-aryl-5-(2'-aminophenyl)-4-hydroxy-1,3-thiazoles. *J Mol Struct* 2019;1175:804-810. <https://doi.org/10.1016/j.molstruc.2018.08.017> (b) Gampe DM, Hansch VG, Schram S, Menzel R, Weiz D, Beckert R. Mixing Chromophores: Donor-Acceptor Dyes with Low-Lying LUMOs and Narrow Band Gaps by Connecting 4-Alkoxythiazoles and Azaacenes. *Eur J Org Chem* 2017;10:1369-1379. <https://doi.org/10.1002/ejoc.201601521> (c) Habenicht SH, Rohland P, Reichel J, Biver T, Minei P, Jakobi D, Pucci A, Weiz D, Beckert R, Görls H. Small Molecules as Long-Wavelength Fluorophores: Push-Pull Substituted 4-Alkoxy-1,3-thiazoles. *Synthesis* 2018;50:303-313. <https://doi.org/10.1055/s-0036-1588581> (d) Habenicht SH, Kupfer S, Nowotny J, Schramm S, Weiz D, Beckert R, Görls H. Highly fluorescent single crystals of a 4-ethoxy-1,3-thiazole. *Dyes pigm* 2018;149:644-651. <https://doi.org/10.1016/j.dyepig.2017.11.016> (e) Kammel R, Tarabova D, Machalický O, Nepras M, Frumarova B, Hanusek J. Synthesis, characterization and spectral properties of new, highly fluorescent, 4-hydroxythiazoles. *Dyes Pigm* 2016;128:101-110. <https://doi.org/10.1016/j.dyepig.2016.01.017> (f) Habenicht SH, Schramm S, Fischer S, Sachse T, Herrmann-Westendorf F, Bellmann F, Dietzek B, Presselt M, Weiß D, Beckert R, Görls H. Tuning the polarity and surface activity of hydroxythiazoles – extending the applicability of highly fluorescent self-assembling chromophores to supra-molecular photonic structures. *J Mater Chem C* 2016;4:958-

971. <https://doi.org/10.1039/C5TC03632A> (g) Habenicht SH, Siegmann M, Kupfer S, Kübel J, Weiß D, Cherek D, Möller U, Dietzek B, Gräfe S, Beckert R. And yet they glow: thiazole based push–pull fluorophores containing nitro groups and the influence of regioisomerism. *Methods Appl Fluoresc* 2015;3:025005. <https://doi.org/10.1088/2050-6120/3/2/025005> (h) Täuscher E, Weiß D, Beckert R, Fabian J, Assumpção A, Görls H. Classical heterocycles with surprising properties: the 4-hydroxy-1,3-thiazoles. *Tetrahedron Lett* 2011;52:2292–2294. <https://doi.org/10.1016/j.tetlet.2011.02.048> (i) Grummt UW, Weiss D, Birckner E, Beckert R. Pyridylthiazoles: Highly Luminescent Heterocyclic Compounds. *J Phys Chem A* 2007;111:1104–1110. <https://doi.org/10.1021/jp0672003> (j) Wrona-Piotrowicz A, Damian Plazuk, Janusz Zakrzewski, Métivier R, Nakatani K, Makal A. Solution-and solid-state emitters with large Stokes shifts combining pyrene and 4-hydroxythiazole fluorophores. *Dyes Pigm* 2015;121:290–298. <https://doi.org/10.1016/j.dyepig.2015.05.030>
- [5] (a) Radhakrishnan R, Sreejalekshmi KG. Computation design, Synthesis, and Structure Property Evaluation of 1,3-Thiazole-Based Color-Tunable Multi-heterocyclic Small Organic Fluorophores as Multifunctional Molecular Materials. *J Org Chem* 2018;7:3453–3466. <https://doi.org/10.1021/acs.joc7b02978>. (b) Murai T, Yamaguchi K, Hayano T, Maruyama T, Kawai K, Kawakami H, Yashita A. Synthesis and Photophysical Properties of 5-*N*-Arylamino-4-methylthiazoles Obtained from Direct C–H Arylations and Buchwald–Hartwig Aminations of 4-Methylthiazole. *Organometallics* 2017;36:2552–2558. <https://doi.org/10.1021/acs.organomet.7b00128> (c) Tao T, Ma BB, Peng YX, Wang XX, Huang W, You XZ. Asymmetrical/Symmetrical D– π –A/D– π –D Thiazole-Containing Aromatic Heterocyclic Fluorescent Compounds Having the Same Triphenylamino Chromophores. *J Org Chem* 2013;78:8669–8679. <https://doi.org/10.1021/jo401384g> (d) Yamaguchi K, Murai N, Hasegawa S, Miwa Y, Kutsumizu S, Maruyama T, Sasamori T, Takitoh N. 5-*N*-Arylaminothiazoles as Highly Twisted Fluorescent Monocyclic Heterocycles: Synthesis and Characterization. *J Org Chem* 2015;80:10742–10756. <https://doi.org/10.1021/acs.joc.5b01963>. (e) Thorat KG, Sekar N. Pyrrole-thiazole based push-pull chromophores: An experimental and theoretical approach to structural, spectroscopic and NLO properties of the novel styryl dyes. *J Photochem Photobiology A* 2017;333:1–17. <https://doi.org/10.1016/j.jphotochem.2016.10.009> (f) Tayade RP, Sekar N. Synthesis of novel thiazole based carbaldehyde as potential sensor for fluoride anion and spectroscopic properties. *J Fluoresc* 2017;27:1117–1128. <https://doi.org/10.1007/s10895-017-2047-9> (g) Tayade RP, Sekar N. Novel thiazole based styryl dyes with benzimidazole unit - synthesis, photophysical and TD-DFT studies. *J Fluoresc* 2017;27:167–180 <https://doi.org/10.1007/s10895-016-1943-8> (h) Shreykar MR, Sekar N. Stimuli-responsive luminescent coumarin thiazole hybrid dye: Synthesis. Aggregation induced emission, thermochromism and DFT study. *Dyes Pigm* 2017;142:121–125. <https://doi.org/10.1016/j.dyepig.2017.03.028> (i) Tayade RP, Sekar N. Benzimidazole-thiazole based NLOphoric styryl dyes with solid state emission – Synthesis, photophysical, hyperpolarizability and TD-DFT studies. *Dyes Pigm* 2016;128:111–123. <https://doi.org/10.1016/j.dyepig.2016.01.012> (j)

- Shreykar MR, Sekar N. Resonance induced proton transfer leading to NIR emission in coumarin thiazole hybrid dyes: Synthesis and DFT insights. *Tetrahedron Lett* 2016;57:4174–4177. <https://doi.org/10.1016/j.tetlet.2016.07.097> (k) Sekar N, Umap PG, Sharad R. Patil Fluorescent Styryl Dyes from 4-Chloro-2-(Diphenylamino)-1,3-Thiazole-5-Carbaldehyde—Synthesis, Optical Properties and TDDFT Computations *J Fluoresc* 2015;25:1787-1800. <https://doi.org/10.1007/s10895-015-1668-0>
- [6] Valeur B, Berberan-Santos MN. *Molecular Fluorescence*. 2nd ed. Weinheim, Germany: Wiley-VCH Verlag & Co.; 2013.
- [7] Wang Y, Yang MY, Zheng MH, Zao XL, Xie YZ, Jin JY. 2-Pyridylthiazole derivative as ICT-based ratiometric fluorescent sensor for Fe(III). *Tetrahedron Lett* 2016;12:2399-2492. <https://doi.org/10.1016/j.tetlet.2016.04.065>
- [8] (a) Nagura K, Saito S, Yusa H, Yamawaki H, Fujihisa H, Sato H, Shimoikeda Y, Yamaguchi S. Distinct responses to mechanical grinding and hydrostatic pressure in luminescent chromism of tetrazolylthiophene. *J Am Chem Soc* 2013;135:0322-10325. <https://doi.org/10.1021/ja4055228> (b) Ozkutuk M, Ipek E, Aydinler B, Mammas S, Seferoglu Z. Synthesis, spectroscopic, thermal and electrochemical studies on thiazolyl azo based disperse dyes bearing coumarin. *J Mol Struct* 2016;1108:521-532. <https://doi.org/10.1016/j.molstruc.2015.12.032>
- [9] Lugovik KI, Popova AV, Eltyshv AK, Benassi E, Belskaya NP. Synthesis of Thiazoles Bearing Aryl Enamine/Aza-enamine Side Chains: Effect of the π -Conjugated Spacer Structure and Hydrogen Bonding on Photophysical Properties. *Eur J Org Chem* 2017;28:4175-4187. <https://doi.org/10.1002/ejoc.201700518>
- [10] (a) Paramonov IV, Belskaia NP, Bakulev VA. Reaction of (Arylhrazono)cyanothioacetamides with Halo Ketones. *Chem Heterocycl Compd* 2003;39:1385–1395. <https://doi.org/10.1023/B:COHC.0000010657.14733.8e> (b) Belskaya NP, Lugovik KI, Ivina AD, Bakulev VA, Fan ZJ. Reaction of enamines and azaenamides containing a thioamide group with dimethyl acetylenedicarboxylate. *Chem Het Compd* 2014;50:888–900. <https://doi.org/10.1023/B:COHC.0000010657.14733.8e> (d) Deryabina TG, Demina MA, Belskaya NP, Bakulev VA. Reaction of 3-aryl-2-cyanothioacrylamides with dimethyl acetylenedicarboxylate, methyl propiolate, and *N*-phenylmaleimide. *Russ Chem Bull* 2005;54:2880–2889. <https://doi.org/10.1007/s11172-006-0204-4> (e) Dotsenko VV, Krivokolysko SG. Regioselective reduction of 2-cyanoprop-2-enethioamides with sodium borohydride. *Russ Chem Bull* 2012;61:2261-2264. <https://doi.org/10.1007/s11172-012-0321-1> (f) Brunskill JSA, De A, Ewing DF. Dimerisation of 3-aryl-2-cyanothioacrylamides. A [2s+4s] cyclo-addition to give substituted 3,4-dihydro-2*H*-thiopyrans. *J Chem Soc Perkin Trans 1* 1978;0:629-633. <https://doi.org/10.1039/P19780000629>
- [11] (a) Wallenfels K, Gellrich M. Über den Mechanismus der Wasserstoffübertragung mit Pyridinnucleotiden, XV Freie Radikale als Reduktionsprodukte von Pyridiniumsalzen. *Liebigs Ann Chem* 1959;621:198-214. <https://doi.org/10.1002/jlac.19596210119> (b) Weiss A, inventor; Clariant

International Ltd, assignee. Use of thiazolyl-pyridinium dyes for optical data recording. US patent 20080108799. 2008 May 08.

- [12] Bashandy MS, Abd El-Gilil SM. Synthesis, molecular docking and anti-human breast cancer activities of novel thiazolylacetonitriles and thiazolylacrylonitriles and their derivatives containing benzenesulfonylpyrrolidine moiety. *Heterocycles* 2016;92:431-469. <https://doi.org/10.3987/COM-15-13384>
- [13] Tani S, Uehara TN, Yamaguchi J, Itami K. Programmed synthesis of arylthiazoles through sequential C–H couplings. *Chem Sci* 2014;5:123-135. <https://doi.org/10.1039/C3SC52199K>
- [14] (a) Langhals H, Potrawa T, Nöth H, Linti G. The Influence of Packing Effects on the Solid-State Fluorescence of Diketopyrrolopyrroles. *Angew Chem Int Ed* 1989;28:478-480. <https://doi.org/10.1002/anie.198904781> (b) Dreuw A, Plötner J, Lorenz L, Wachtveitl J, Djanhan JE, Brüning J, Metz T, Bolte M, Schmidt MU. Molecular Mechanism of the Solid-State Fluorescence Behavior of the Organic Pigment Yellow 101 and Its Derivatives. *Angew Chem Int Ed* 2005;44:7783–7786. <https://doi.org/10.1002/anie.200501781>
- [15] (a) Choi S, Bouffard J, Kim Y. Aggregation-induced emission enhancement of a meso-trifluoromethyl BODIPY via J-aggregation. *Chem Sci* 2014;5:751-755. <https://doi.org/10.1039/C3SC52495G> (b) Xie Z, Yang B, Liu L, Ma Y. J-type dipole stacking and strong π - π interactions in the crystals of distyrylbenzene derivatives: the crystal structures, high luminescence properties and prediction of high mobility. *J Mol Eng Mater* 2013;1:2251-2373. <https://doi.org/10.1142/S2251237313400029>
- [16] (a) Cornil J, dos Santos DA, Crispin X, Silbey R, Brédas JL. Influence of Interchain Interactions on the Absorption and Luminescence of Conjugated Oligomers and Polymers: A Quantum-Chemical Characterization. *J Am Chem Soc* 1998;120:1289-1299. <https://doi.org/10.1021/ja973761j> (b) Liu J, Meng L, Zhu W, Zhang C, Zhang H, Yao Y, Wang Z, He P, Zhang X, Wang Y, Zhen Y, Dong H, Yia Y, Hu W. A cross-dipole stacking molecule of an anthracene derivative: integrating optical and electrical properties. *J Mater Chem C* 2015;3:3068-3071. <https://doi.org/10.1039/C4TC02964J> (c) Kamiński DM, Hoser AA, Gagoś M, Matwijczuk A, Arczewska M, Niewiadomy A, Woźniak K. Solvatomorphism of 2-(4-fluorophenylamino)-5-(2,4-dihydroxybenzeno)-1,3,4-thiadiazole chloride. *Cryst Growth Des* 2010;10:3480-3488. <https://doi.org/10.1021/cg1003319>
- [17] (a) Horvath P, Sebej P, Solomek T, Klan P. Small-Molecule Fluorophores with Large Stokes Shifts: 9-Iminopyronin Analogues as Clickable Tags. *J Org Chem* 2015;80:1299-1311. <https://doi.org/10.1021/jo502213t> (b) Li JZ, Leng TH, Wang ZQ, Zhou L, Gong XQ, Shen YJ, Wang CU. A Large stokes shift, sequential colorimetric fluorescent probe for sensing $\text{Cu}^{2+}/\text{S}^{2-}$ and its applications. *J Photochem Photobiol A* 2019;373:146-153. <https://doi.org/10.1016/j.jphotochem.2019.01.006> (c) Araneda JF, Piers WE, Heyne D, Parvez M,

McDonald R. High Stokes Shift Anilido-Pyridine Boron Difluoride Dyes. *Angew Chem Int Ed* 2011;50:12214-12217. <https://doi.org/10.1002/anie.201105228>

[18] (a) Zhao YS. *Organic nanophotonics: fundamentals and applications*. Heidelberg: Springer; 2014. (b) Monalti M, Credi A, Prodi L, Gandolfi MT. *Handbook of Photochemistry*. 3rd ed. Boca Raton: CRC Press; 2006.

[19] (a) Kim E, Lee Y, Lee S, Park SB. Discovery, Understanding, and Bioapplication of Organic Fluorophore: A Case Study with an Indolizine-Based Novel Fluorophore, Seoul-Fluor. *Acc Chem Res* 2015;48:538-547. <https://doi.org/10.1021/ar500370v> (b) Goncalves MST. Fluorescent Labeling of Biomolecules with Organic Probes. *Chem Rev* 2009;109:190-212. <https://doi.org/10.1021/cr0783840>

- Fluorescent thiazoles sensitive to microenvironment were designed and synthesized.
- The compounds demonstrated the large Stokes shift and significant quantum yield.
- Relationship between structure and fluorescent characteristics was established.
- Insertion of acrylonitrile group enhances the fluorescence of the thiazoles.
- The basis for the synthesis of new extra sensitive thiazoles was created.